# Quantum simulations of strongly coupled quark-gluon plasma

V.S. Filinov,[1,*] Yu.B. Ivanov,[2,3] M. Bonitz,[4] P.R. Levashov,[1] and V.E. Fortov[1]

[1] *Joint Institute for High Temperatures, Russian Academy of Sciences, Moscow, Russia*
[2] *GSI Helmholtzzentrum für Schwerionenforschung, Darmstadt, Germany*
[3] *Kurchatov Institute, Moscow, Russia*
[4] *Institute for Theoretical Physics and Astrophysics, Christian Albrechts University, Kiel, Germany*

A strongly coupled quark-gluon plasma (QGP) of constituent quasiparticles is studied by a path-integral Monte-Carlo method. This approach is a quantum generalization of the model developed by Gelman, Shuryak and Zahed. It is shown that this method is able to reproduce the QCD lattice equation of state, internal energy, entropy and trace anomaly and also yields valuable insight into the internal structure of the QGP. The results indicate that the QGP reveals liquid-like rather than gas-like properties.

## I. INTRODUCTION

Investigation of properties of the QGP is one of the main challenges of strong-interaction physics, both theoretically and experimentally. Many features of this matter were experimentally discovered at the Relativistic Heavy Ion Collider (RHIC) at Brookhaven. The most striking result, obtained from analysis of these experimental data [1], is that the deconfined quark-gluon matter behaves as an almost perfect fluid rather than a perfect gas, as it could be expected from the asymptotic freedom.

There are various approaches to studying QGP. Each approach has its advantages and disadvantages. The most fundamental way to compute properties of the strongly interacting matter is provided by the lattice QCD [2, 3]. Interpretation of these very complicated computations requires application of various QCD motivated, albeit schematic, models simulating various aspects of the full theory. Moreover, such models are needed in cases when the lattice QCD fails, e.g. at large baryon chemical potentials and out of equilibrium. While some progress has been achieved in the recent years, we are still far away from having a satisfactory understanding of the QGP dynamics.

A semi-classical approximation, based on a point like quasiparticle picture has been introduced in [4]. It is expected that the main features of non-Abelian plasmas can be understood in simple semi-classical terms without the difficulties inherent to a full quantum field theoretical analysis. Independently the same ideas were implemented in terms of molecular dynamics (MD) [5]. Recently this MD approach was further developed in a series of works [6, 7]. The MD allowed one to treat soft processes in the QGP which are not accessible by perturbative means.

A strongly correlated behavior of the QGP is expected to show up in long-ranged spatial correlations of quarks and gluons which, in fact, may give rise to liquid-like and, possibly, solid-like structures. This expectation is based on a very similar behavior observed in electrodynamic plasmas [6, 8, 9]. This similarity was exploited to formulate a classical nonrelativistic model of a color Coulomb interacting QGP [6] which was numerically analyzed by classical MD simulations. Quantum effects were either neglected or included phenomenologically via a short-range repulsive correction to the pair potential. Such a rough model may become a critical issue at high densities, where quantum effects strongly affects properties of the QGP. Similar models have been used in electrodynamic plasmas and showed poor behavior in the region of strong wave function overlap, in particular at the Mott density. For temperatures and densities of the QGP considered in [6] these effects are very important as the quasiparticle thermal wave length is of order the average interparticle distance.

In this paper we extend previous classical nonrelativistic simulations [6] based on a color Coulomb interaction to the quantum regime. We develop an approach based on path integral Monte Carlo (PIMC) simulations of the strongly coupled QGP which self-consistently takes into account the Fermi (Bose) statistics of quarks (gluons). Following an idea of Kelbg [10], quantum corrections to the pair potential are rigorously derived[1]. To extend the method of quantum potentials to a stronger coupling, an "improved Kelbg potential" was derived, which contains a single free parameter, being fitted to the exact solution of the quantum-mechanical two-body problem. Thus, the method of the improved Kelbg potential is able to describe thermodynamic properties up to moderate couplings [12]. However, this approach may fail, if bound states of more than two particles are formed in the system. This results in a break-down of the

*Corresponding author E-mail: vladimir_filinov@mail.ru

[1] The idea to use a Kelbg-type effective potential also for quark matter was independently proposed by K. Dusling and C. Young [11]. However, their potentials are limited to weakly nonideal systems.

pair approximation for the density matrix, as demonstrated in [12]. A superior approach, which does not have this limitation, consists in use the original Kelbg potential in the PIMC simulations which effectively map the problem onto a high-temperature weakly coupled and weakly degenerate one. This allows one to rigorously extend the analysis to strong couplings and is, therefore, a relevant choice for the present purpose.

This method has been successfully applied to strongly coupled electrodynamic plasmas [13, 14]. Examples are partially-ionized dense hydrogen plasmas, where liquid-like and crystalline behavior was observed [15, 16]. Moreover, also partial ionization effects and pressure ionization could be studied from first principles [17]. The same methods have been also applied to electron-hole plasmas in semiconductors [18, 19], including excitonic bound states, which have many similarities to the QGP due to smaller mass differences as compared to electron-ion plasmas.

The main goal of this article is to test the developed approach for ability to reproduce known lattice data [2] and to predict other properties of the QGP, which are still unavailable for the lattice calculations. To this end we use a simple model [6] of the QGP consisting of quarks, antiquarks and gluons interacting via a color Coulomb potential. First results of applications of the PIMC method to study of thermodynamic properties of the nonideal QGP have already been briefly reported in [20, 21]. In this paper we present a comprehensive report on the thermodynamic properties.

## II. THERMODYNAMICS OF QGP

### A. Basics of the model

Our model is based on a resummation technique and lattice simulations for dressed quarks, antiquarks and gluons interacting via the color Coulomb potential. The assumptions of the model are similar to those of [6]:

**I.** Quasiparticles masses ($m$) are of order or higher than the mean kinetic energy per particle. This assumption is based on the analysis of lattice data [22, 23]. For instance, at zero net-baryon density it amounts to $m \geq T$, where $T$ is a temperature.

**II.** To take into account relativistic effects the kinetic part of the full quasiparticles energy is described by the relativistic expression.

**III.** Interparticle interaction is dominated by a color-electric Coulomb potential, see Eq. (1).

**IV.** Relying on the fact that the color representations are large, the color operators are substituted by their average values, i.e. by Wong's classical color vectors (8D in SU(3)) with two Casimir conditions [24].

**V.** We consider the $[2+1]$ flavor quark model. Since the masses of the 'up', 'down' and 'strange' quark and antiquark quasiparticles extracted from lattice data are very similar we assume that their masses ($m_q^{\tilde{f}} = m_{\bar{q}}^{\tilde{f}'}; \tilde{f}, \tilde{f}' =$ 'up', 'down' and 'strange') and fractions (1/3) to be equal. However we account for the quark color and flavors in the proper consideration of Fermi statistics effects. Let us stress that gluon quasiparticles obey the Bose statistics and their masses are independent from masses of quark quasiparticles.

The quality of these approximations and their limitations were discussed in [6]. Thus, this model requires the following quantities as a function of temperature and chemical potential as an input:

**1.** the quasiparticle masses, $m$, and

**2.** the coupling constant $g^2$.

All the input quantities should be deduced from the lattice data or from an appropriate model simulating these data.

### B. Path-Integral Monte-Carlo Simulations

Thus, we consider a many-component QGP consisting of $N_g$ dressed gluon quasiparticles and of equal flavor fractions the dressed quarks (with whole number $N_q$) and antiquarks (with whole number $N_{\bar{q}}$) represented by color quasiparticles. In thermal equilibrium to take into account the processes of creation and annihilation the average values of these numbers and their fluctuations can be found in the grand canonical ensemble defined by the chemical

potential and temperature dependent Hamiltonian, which can be written as $\hat{H} = \hat{K} + \hat{U}$. The kinetic and color Coulomb interaction energy of the quasiparticles are

$$\hat{K} = \sum_i \sqrt{p_i^2 + m_i^2(T,\mu_q)} \qquad \hat{U}_C = \frac{1}{2}\sum_{i,j} \frac{g^2(|r_i - r_j|, T, \mu_q)\langle Q_i|Q_j\rangle}{4\pi|r_i - r_j|}, \tag{1}$$

Here $i = 1, \ldots, N_q + N_{\bar{q}} + N_g$, the $Q_i$ denote the Wong's color variable (8-vector in the $SU(3)$ group), $T$ is the temperature and $\mu_q$ is the quark chemical potential, $\langle Q_i|Q_j\rangle$ denote scalar product of color vectors. In fact, the quasiparticle mass and the coupling constant, as deduced from the lattice data, are functions of $T$ and, in general, $\mu_q$. Moreover, $g^2$ is a function of distance $r$, which produces a linearly rising potential at large $r$ [25].

The thermodynamic properties in the grand canonical ensemble with given temperature $T$, chemical potential $\mu_q$ and fixed volume $V$ are fully described by the grand partition function

$$Z\left(\mu_q, \beta, V\right) = \sum_{N_q, N_{\bar{q}}, N_g} \frac{\exp(\mu_q(N_q - N_{\bar{q}})/T)}{N_q! N_{\bar{q}}! N_g!} \sum_\sigma \int_V dr dQ\, \rho(r, Q, \sigma, f; N_q, N_{\bar{q}}, N_g; \beta), \tag{2}$$

where $\rho(r, Q, \sigma, f; N_q, N_{\bar{q}}, N_g; \beta)$ denotes the diagonal matrix elements of the density matrix operator $\hat{\rho} = \exp(-\beta\hat{H})$, and $\beta = 1/T$. Here $\sigma$, $r$ and $Q$ denote the spin, spatial and color degrees of freedom of all quarks, antiquarks and gluons, while $f$ is flavor degrees of freedom of all quarks and antiquarks in the ensemble, respectively. Values of flavor index are defined by the fixed fraction of related numbers of quark and antiquark quasiparticles (see position $V$ in the model description). Correspondingly, the $\sigma$ summation and integration $drdQ$ run over all individual degrees of freedom of the particles. Since the masses and the coupling constant depend on the temperature and chemical potential, special care should be taken to preserve thermodynamical consistency of this approach. In order to preserve the thermodynamical consistency, thermodynamic functions such as pressure, $P$, entropy, $S$, baryon number, $N_B$, and internal energy, $E$, should be calculated through respective derivatives of the logarithm of the partition function

$$\begin{aligned} P &= \partial(T\ln Z)/\partial V, \qquad & S &= \partial(T\ln Z)/\partial T, \\ N_B &= (1/3)\partial(T\ln Z)/\partial\mu_q, \qquad & E &= -PV + TS + 3\mu_q N_B. \end{aligned} \tag{3}$$

This is a conventional way of maintaining the thermodynamical consistency in approaches of the Ginzburg–Landau type as they are applied in high-energy physics.

The exact density matrix $\rho = e^{-\beta\hat{H}}$ of interacting quantum systems can be constructed using a path integral approach [26, 27] based on the operator identity $e^{-\beta\hat{H}} = e^{-\Delta\beta\hat{H}} \cdot e^{-\Delta\beta\hat{H}} \ldots e^{-\Delta\beta\hat{H}}$, where the r.h.s. contains $n+1$ identical factors with $\Delta\beta = \beta/(n+1)$. which allows us to rewrite[2] the integral in Eq. (2)

$$\begin{aligned} &\sum_\sigma \int dr^{(0)} dQ^{(0)}\, \rho(r^{(0)}, Q^{(0)}, \sigma, f; N_q, N_{\bar{q}}, N_g; \beta) = \\ &= \int dr^{(0)} dQ^{(0)} dr^{(1)} dQ^{(1)} \ldots dr^{(n)} dQ^{(n)}\, \rho^{(1)} \cdot \rho^{(2)} \ldots \rho^{(n)} \times \\ &\times \sum_\sigma \sum_{P_q} \sum_{P_{\bar{q}}} \sum_{P_g} (-1)^{\kappa_{P_q} + \kappa_{P_{\bar{q}}}} \mathcal{S}(\sigma, \hat{P}_q \hat{P}_{\bar{q}} \hat{P}_g \sigma')\, \hat{P}_q \hat{P}_{\bar{q}} \hat{P}_g \rho^{(n+1)}\big|_{r^{(n+1)} = r^{(0)}, \sigma' = \sigma} = \\ &= \int dQ^{(0)} dr^{(0)} dr^{(1)} \ldots dr^{(n)}\, \tilde{\rho}(r^{(0)}, r^{(1)}, \ldots r^{(n)}; Q^{(0)}, f^{(0)}; N_q, N_{\bar{q}}, N_g; \beta). \end{aligned} \tag{4}$$

The spin gives rise to the spin part of the density matrix ($\mathcal{S}$) with exchange effects accounted for by the permutation operators $\hat{P}_q$, $\hat{P}_{\bar{q}}$ and $\hat{P}_g$ acting on the quark, antiquark and gluon color $Q^{(n+1)}$, flavor $f^{(n+1)}$ and spatial $r^{(n+1)}$ coordinates, as well as on the spin projections $\sigma'$. The sum runs over all permutations with parity $\kappa_{P_q}$ and $\kappa_{P_{\bar{q}}}$. In Eq. (4) the index $l = 1 \ldots n+1$ labels the off-diagonal density matrices $\rho^{(l)} \equiv \rho\left(r^{(l-1)}, Q^{(l-1)}, f^{(l-1)}; r^{(l)}, Q^{(l)}, f^{(l)}; \Delta\beta\right) \approx \langle r^{(l-1)}|e^{-\Delta\beta\hat{H}}|r^{(l)}\rangle \delta_\epsilon(Q^{(l-1)} - Q^{(l)}) \delta_{f^{(l-1)}, f^{(l)}}$, where $\delta_\epsilon(Q^{(l-1)} - Q^{(l)})$ is a delta-function at $\epsilon \to 0$, while $\delta_{f^{(l-1)}, f^{(l)}}$ is the Kronecker's delta . Accordingly each $a$ particle is represented by a set of $n+1$ coordinates ("beads"), i.e. by $(n+1)$ 3-dimensional vectors $\{r_a^{(0)}, \ldots r_a^{(n)}\}$, flavor index $f^{(0)}$ and a

[2] For the sake of notation convenience, we ascribe superscript $^{(0)}$ to the original variables.

8-dimensional color vector $Q^{(0)}$ in the $SU(3)$ group, since all beads are characterized by the same flavor and color charge.

The main advantage of decomposition (4) is that it allows us to use perturbation theory to obtain approximation for density matrices $\rho^{(l)}$, which is applicable due to smallness of artificially introduced factor $1/(n+1)$. From physical point of view this means that the characteristic distance between subsequent "beads" $r_a^{(l-1)}$ and $r_a^{(l)}$ for each particle in Eq. (4) can be always made smaller then a characteristic scale of variation of the potential energy. Each factor in (4) should be calculated with the accuracy of order of $1/(n+1)^\theta$ with $\theta > 1$, as in this case the error of the whole product in the limit of large $n$ will be equal to zero. In the limit $(n+1) \longrightarrow \infty$ $\rho^l$ can be approximated by a product of two-particle density matrices. Generalizing the electrodynamic plasma results [14] to the case of an additional bosonic species (i.e. gluons), we write

$$\tilde{\rho}(r^{(0)}, r^{(1)}, \dots r^{(n)}; Q^{(0)}, f^{(0)}; N_q, N_{\bar{q}}, N_g; \beta) =$$
$$= \sum_{s,k} \frac{C^s_{N_q}}{2^{N_q}} \frac{C^k_{N_{\bar{q}}}}{2^{N_{\bar{q}}}} \frac{\exp\{-\beta U(r,Q,\beta)\}}{\tilde{\lambda}_q^{3N_q} \tilde{\lambda}_{\bar{q}}^{3N_{\bar{q}}} \tilde{\lambda}_g^{3N_g}} \ \mathrm{per}\, ||\tilde{\phi}^{n,0}||_{\mathrm{glue}} \det ||\tilde{\phi}^{n,0}||_s \det ||\tilde{\phi}^{n,0}||_k \prod_{l=1}^{n} \prod_{p=1}^{N} \phi^l_{pp}\,, \tag{5}$$

where $N = N_q + N_{\bar{q}} + N_g$, $s$ and $k$ are numbers of quarks and antiquarks, respectively, with the same spin projection, $\widetilde{\lambda}_a^3 = \lambda_a^3 \sqrt{0.5\pi/(\beta m)^5}$; $\lambda_a = \sqrt{2\pi\beta/m_a}$ is a thermal wavelength of an $a$ particle, $C^s_{N_a} = N_a!/[s!(N_a - s)!]$, the antisymmetrization and symmetrization are taken into account by the symbols "det" and "per" denoting the determinant and permanent, respectively.

For $z_p = \Delta\beta m_p(T,\mu_q)\sqrt{1 + 2\pi \left|\xi_p^{(l)}\right|^2} / \Delta\beta m_p(T,\mu_q)$ functions $\phi^l_{pp}$ proportional to off-diagonal matrix elements of one particle relativistic density matrices are defined by $\phi^l_{pp} \equiv K_2(z_p)/z_p^2$, while matrix elements $\tilde{\phi}^{n,0}_{to} = K_2(z^{n,0}_{to})/(z^{n,0}_{to})^2 \delta_\epsilon(Q_t - Q_o)\delta_{f_t,f_o}$ depend on $z^{n,0}_{to} = \Delta\beta m_t(T,\mu_q)\sqrt{1 + 2\pi \left|(r_t^{(0)} - r_o^{(0)}) + y_t^{(n)}\right|^2} / (\Delta\lambda_a^2 \Delta\beta m_t(T,\mu_q))$. Here $t$ and $o$ are particle's indexes, $K_2(z)$ are modified Bessel functions with arguments expressed in terms of distances $(y_a^{(1)}, \dots, y_a^{(n)})$ and dimensionless distances $(\xi_a^{(1)}, \dots, \xi_a^{(n)})$ between neighboring beads of an $a$ particle, defined as $r_a^{(l)} = r_a^{(0)} + y_a^{(l)}$, $(l > 0)$, and $y_a^{(l)} = \Delta\lambda_a \sum_{k=1}^{l} \xi_a^{(k)}$ and $\Delta\lambda_a = \sqrt{2\pi\Delta\beta/m_a}$. Notice that the indices $s$ and $k$ in $\det ||\tilde{\phi}^{n,0}||_s$ and $\det ||\tilde{\phi}^{n,0}||_k$ denoted that matrices $||\tilde{\phi}^{n,0}||$ have nonzero blocks related to quark and antiquark quasiparticles with the same flavor and spin projections. The main contribution to the partition function comes from configurations in which the "size" of the cloud of beads of quasiparticles is of the order of $1/m(T,\mu_q)$ providing spatial quasiparticle localization.

The density matrix (5) has been transformed to a form which does not contain an explicit sum over permutations and thus no sum of terms with alternating sign (in the case of quarks and antiquarks). Let us stress that the determinants depend also on the flavor and color variables.

In Eq. (5) the total color interaction energy

$$U(r,Q,\beta) = \frac{1}{n+1} \sum_{l=1}^{n+1} \tilde{U}^{(l)} = \frac{1}{n+1} \sum_{l=1}^{n+1} \frac{1}{2} \sum_{p \neq t} \Phi^{pt}(|r_p^{(l-1)} - r_t^{(l-1)}|, |r_p^{(l)} - r_t^{(l)}|, Q_p, Q_t) \tag{6}$$

is defined in terms of off-diagonal two-particle effective quantum potential $\Phi^{pt}$, which is obtained by expanding the two-particle density matrix $\rho_{pt}$ up to the first order in small parameters $1/(n+1)$:

$$\rho_{pt}(r,r',Q_p,Q_t,\Delta\beta) \approx \rho^0_{pt}(r,r',Q_p,Q_t,\Delta\beta) - \int_0^1 d\tau \int dr'' \frac{\Delta\beta g^2(|r''|,T,\mu_q)\langle Q_p|Q_t\rangle}{4\pi|r''|\Delta\lambda^2_{pt}\sqrt{\tau(1-\tau)}}$$
$$\times \ \exp\left(-\frac{\pi|r' - r''|^2}{\Delta\lambda^2_{pt}(1-\tau)}\right) \exp\left(-\frac{\pi|r'' - r|^2}{\Delta\lambda^2_{pt}\tau}\right) \approx \rho^0_{pt} \exp[-\Delta\beta\Phi^{pt}(r,r',Q_p,Q_t)], \tag{7}$$

where $\rho^0$ is nonrelativistic one particle density matrix, $r = r_p - r_t$, $r' = r'_p - r'_t$, $\Delta\lambda_{pt} = \sqrt{2\pi\Delta\beta/m_{pt}}$, $m_{pt} = m_p m_t/(m_p + m_t)$ is the reduced mass of the $(pt)$-pair of particles, and $\rho^0_{pt}$ is the ideal two-particle density matrix. The result for the diagonal color Kelbg potential can be written as

$$\Phi^{pt}(r,r,Q_p,Q_t) \approx \frac{g^2(T,\mu_q)\,\langle Q_p|Q_t\rangle}{4\pi\Delta\lambda_{pt}x_{pt}} \left\{1 - e^{-x^2_{pt}} + \sqrt{\pi}x_{pt}\left[1 - \mathrm{erf}(x_{pt})\right]\right\}, \tag{8}$$

where $x_{pt} = |r_p - r_t|/\Delta\lambda_{pt}$. Here the function $g^2(T,\mu_q) = \overline{g^2(r'',T.\mu_q)}$, resulting from averaging of the initial $g^2(r'',T,\mu_q)$ over relevant distances of order $\Delta\lambda_{pt}$, plays the role of an effective coupling constant. Note that the color

Kelbg potential approaches the color Coulomb potential at distances larger than $\Delta\lambda_{pt}$. What is of prime importance, the color Kelbg potential is finite at zero distance, thus removing in a natural way the classical divergences and making any artificial cut-offs obsolete. This potential is a straightforward generalization of the corresponding potential of electrodynamic plasmas [12]. The off-diagonal elements of the effective interaction are approximated by the diagonal one by means of $\Phi^{pt}(r,r';,Q_p,Q_t) \approx [\Phi^{pt}(r,r,Q_p,Q_t) + \Phi^{pt}(r',r',Q_p,Q_t)]/2$.

## III. SIMULATIONS OF QGP

To test the developed approach we consider the QGP only at zero baryon density. Ideally the parameters of the model should be deduced from the QCD lattice data. However, presently this task is still quite ambiguous. Therefore, in the present simulations we take a possible set of parameters. The phenomenologic QCD estimations [**?** ] of coupling constant, i.e. $\alpha_s = g^2/(4\pi)$, used in the simulations is displayed in the left panel of Fig. 1. The $T$-dependence of quasiparticle mass used in this work is also presented in Fig. 1 (left panel). The right panel presents the calculated in grand canonical ensemble the temperature dependences of the interparticle average distance (Wigner-Seitz radius $r_s^3 = (3/4\pi n)$, n is the density of all quasi particles. The quark quasiparticles degeneracy parameter $\chi = n_q\lambda_q^3$ and the plasma coupling parameter $\Gamma$ are defined as:

$$\Gamma = \frac{\overline{q_2} g^2}{4\pi r_s T}, \tag{9}$$

where $\overline{q_2}$ the quadratic Casimir value averaged over quarks, antiquarks and gluons, $\overline{q_2} = N_c^2 - 1$ is a good estimate for this quantity. The plasma coupling parameter is a measure of ratio of the average potential to the average kinetic energy. It turns out that $\Gamma$ is larger the unity which indicates that the QGP is a strongly coupled Coulomb liquid rather than a gas. In the studied temperature range, $1 < T/T_c < 3$, the QGP is, in fact, quantum degenerate, since the

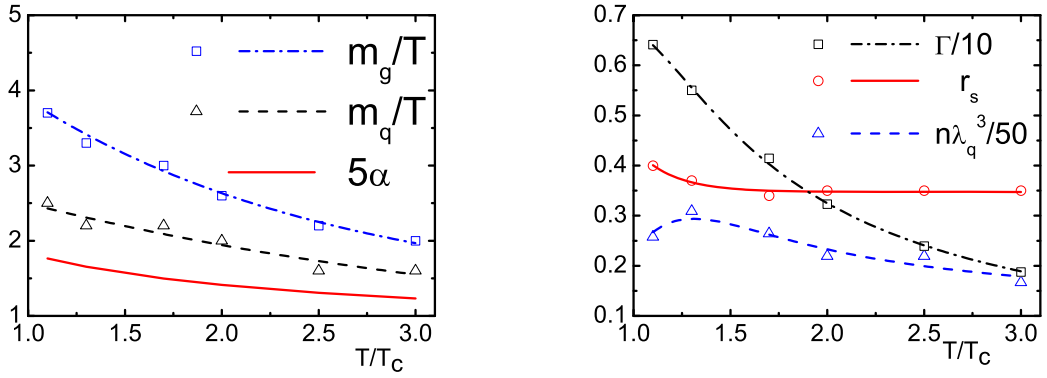


Рис. 1: Left panel:Temperature dependences of the model input quantities: the coupling constant $\alpha_s$ (scaled by 5) and quasiparticle mass-to-temperature ratio. Right panel: Temperature dependences of the calculated interparticle average distance $r_s$ (Wigner-Seitz radius) and related the quark quasiparticles degeneracy parameter $\chi$ and the plasma coupling parameter $\Gamma$ [see Eq. (9)]. The degeneracy parameters for different species does not coincide, since the quasiparticle masses are different.

degeneracy parameter $\chi = n_q\lambda_q^3$ (where the thermal wave length $\lambda_q$ was defined in the previous sect.) varies from 50 to 5, see Fig. 1 (right panel). The degeneracy parameters for different species does not coincide, since the quasiparticle masses are different.

Calculation of the equation of state (Fig. 2) was used to optimize the parameters of the model in order to proceed to predictions of other properties concerning the internal structure and in the future also non-equilibrium dynamics of the QGP.

Figure 3 additionally presents the entropy ($S$) and trace anomaly ($\varepsilon - 3P$) of the QGP computed in the PIMC method. These quantities are calculated accordingly to Eqs. (3). In order to avoid the numeric noise, the derivative of a smooth interpolation between the PIMC points (Fig. 2) was taken. These results are compared to lattice data of [2, 3]. It is not surprising that agreement with the lattice data is also good, since it is a direct consequence of the good reproduction of the pressure.

Details of our path integral Monte-Carlo simulations have been discussed elsewhere in a variety of papers and review articles, see, e.g. [28] and references therein. The main idea of the simulations consists in constructing a Markov process

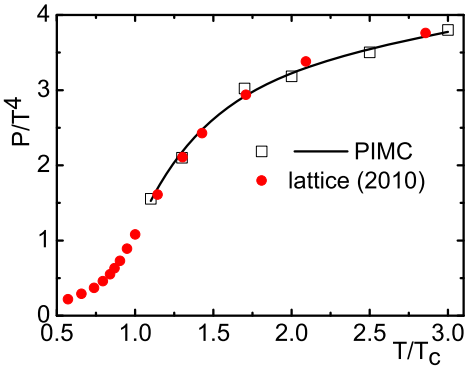


Рис. 2: Equation of state (pressure versus temperature) of the QGP from PIMC simulations (open squares) compared to lattice data of [2, 3]. The solid line is a smooth interpolation between the PIMC points.

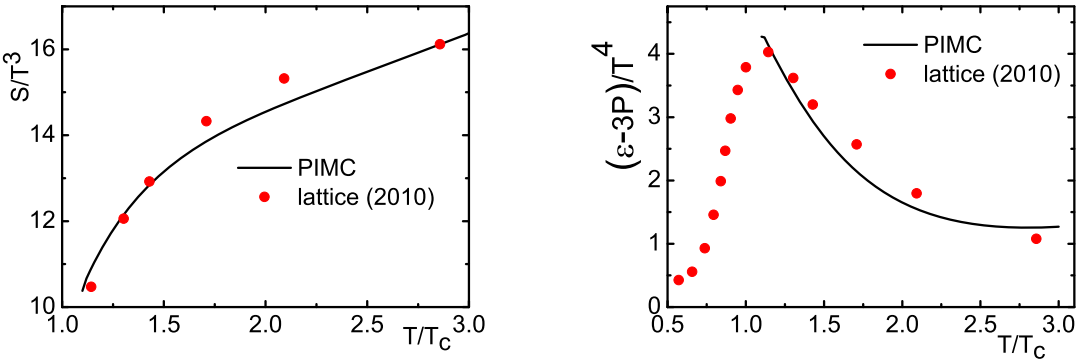


Рис. 3: Entropy (left panel) and trace anomaly (right panel) of the QGP from PIMC simulations (solid line) compared to lattice data of [2, 3]. Notation is the same as in the right panel of Fig. 2.

of configurations which differ by the particle coordinates. Additionally to the case of electrodynamic plasmas, here we randomly sample, according to the group measure, the color variables $Q$ of all particles until convergence is achieved. We use a cubic simulation box with periodic boundary conditions. The number of particles was taken as $N = N_q + N_{\bar{q}} + N_g = 40 + 40 + 40 = 120$, and the number of beads, $n = 20$.

Let us now consider the spatial arrangement of the quasiparticles in the QGP by studying the pair distribution functions (PDF's) $g_{ab}(r)$. They give the probability density to find a pair of particles of types $a$ and $b$ at a certain distance $r$ from each other and are defined as

$$g_{ab}(R_1 - R_2) = \frac{1}{Z N_q! N_{\bar{q}}! N_g!} \sum_{\sigma} \int dr dQ\, \delta(R_1 - r_1^a)\delta(R_2 - r_2^b)\rho(r, Q, \sigma; \beta). \tag{10}$$

The PDF's depend only on the difference of coordinates because of the translational invariance of the system. In a non-interacting classical system, $g_{ab}(r) \equiv 1$, whereas interactions and quantum statistics result in a re-distribution of the particles. Results for the PDF's at temperatures $T/T_c = 3$ and $T/T_c = 1.1$ are shown in the panels of Fig. 4.

At distances, $r/\sigma \geq 0.2$, all PDF's of particles (Fig. 4) coincide. A drastic difference in the behavior of the PDF's of quarks and gluons (the anti-quark PDF is identical to the quark PDF) occurs at distances $r/\sigma \leq 0.2$. Here the gluon PDF increases monotonically when the distance goes to zero, while the PDF of quarks (and antiquarks) are practically equal to one. This difference is the effect of the quantum statistics. The enhanced population of low distance states of gluons is due to Bose statistics and the color-Coulomb attraction. In contrast, the weak variation of PDF for quarks at the small distance range is a consequence of high degeneracy, as masses of quark and antiquark quasiparticles are several time smaller. In an ideal Fermi gas $g(r)$ for particles with different flavor, colors and/or opposite spins the PDF equals unity in the limit $r \to 0$. Oscillations of the PDF at very small distances of order $r \leq 0.1\sigma$ are related to Monte Carlo statistical error, as probability of quasiparticles being at short distances quickly decreases.

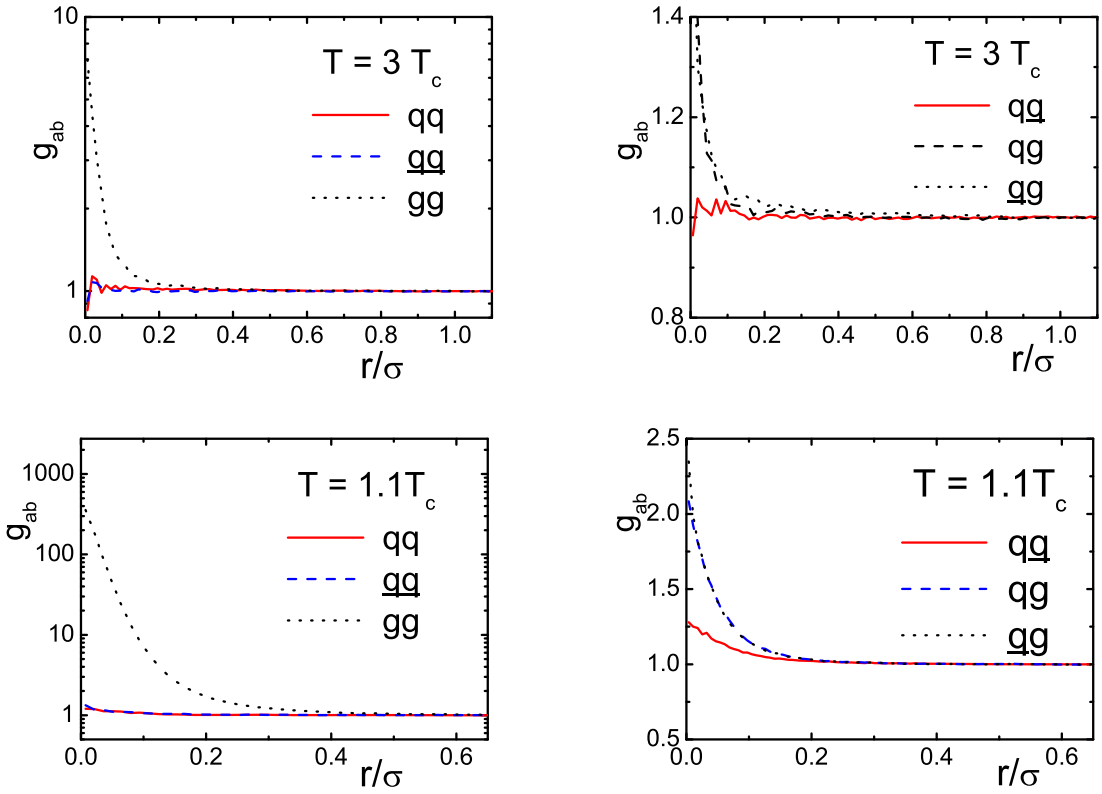


Рис. 4: Pair distribution functions of identical (left panels) and different (right panels) quasiparticles at temperatures $T/T_c = 3$ (upper panels) and $T/T_c = 1.1$ (lower panels). The distance is measured in units of $\sigma = 1/T_c = 1.1$ fm.

At small distances, $r \leq 0.2\sigma$, a strong increase is observed in all PDF's of quark-gluon particles (right panel of Fig. 4), which resembles the behavior of the gluon-gluon PDF. Strong enhancement of PDF functions is connected with more strong interaction with gluon quasiparticles, as quadratic Casimir for gluons is much more than the same value for quarks. This increase is also a clear manifestation of an effective pair attraction. This attraction suggests that the color vectors of nearest neighbors of any type are anti-parallel.

Thus, at $T/T_c = 3$ we observe signs of a spatial ordering, cf. the peak of the quark PDF around $r/\sigma = 0.1 - 0.2$, which may be interpreted as emergence of liquid-like behavior of the QGP. Much more pronounced is the short-range structure of nearest neighbors. The QGP lowers its total energy by minimizing the color Coulomb interaction energy via a spontaneous "anti-ferromagnetic" ordering of color vectors. This gives rise to a clustering of quarks, antiquarks and gluons. To verify the relevance of these trends, a more refined spin-resolved analysis of the PDF's and CPDF's is necessary, together with simulations in a broader range of temperatures which are presently in progress.

## IV. CONCLUSION

Quantum Monte Carlo simulations based on the quasiparticle picture of the QGP are able to reproduce the lattice equation of state (even near the critical temperature) and also yield valuable insight into the internal structure of the QGP. Our results indicate that the QGP reveals liquid-like (rather than gas-like) properties even at the highest considered temperature of $3T_c$.

Our analysis is still simplified and incomplete. It is still confined only to the case of zero baryon chemical potential. The input of the model also requires refinement. Work on these problems is in progress.

However, the PIMC method is not able to yield dynamical and transport properties of the QGP. One way to achieve this is to develop semiclassical color molecular dynamics simulations. In contrast to previous MD simulations [6], where quantum effects were included phenomenologically via a short range potential, we have developed a more rigorous approach to study the dynamical and transport properties of strongly coupled quark-gluon systems which is based on the combination of the Feynman and Wigner formulation of quantum dynamics. The basic ideas of this

approach for the electron-ion plasmas have been published in [29]. In particular, this approach allows us to deduce the viscosity of the QGP. Work on these problems is also in progress.

We acknowledge stimulating discussions with D. Blaschke, R. Bock, B. Friman, C. Ewerz, D. Rischke, and H. Stoecker. Y.I. was partially supported by the Deutsche Forschungsgemeinschaft (DFG projects no. 436 RUS 113/558/0-3 and no. WA 431/8-1), the RFBR grant no. 09-02-91331 NNIO_a, and grant no. NS-7235.2010.2.

[1] E. Shuryak, Prog. Part. Nucl. Phys. **62**, 48 (2009).
[2] Z. Fodor and S. D. Katz, arXiv:0908.3341 [hep-ph].
[3] S. Borsanyi, G. Endrodi, Z. Fodor, A. Jakovac, S. D. Katz, S. Krieg, C. Ratti, K. K. Szabo, JHEP 1011:077,2010
[4] D. F. Litim and C. Manuel, Phys. Rev. Lett. **82**, 4981 (1999); Nucl.Phys. B **562**, 237 (1999); Phys. Rev. D **61**, 125004 (2000); Phys. Rep. **364**, 451 (2002).
[5] M. Hofmann, M. Bleicher, S. Scherer, *et al.*, Phys. Lett. B **478**, 161 (2000).
[6] B. A. Gelman, E. V. Shuryak, and I. Zahed, Phys. Rev. C **74**, 044908 (2006); **74**, 044909 (2006).
[7] S. Cho and I. Zahed, Phys. Rev. C **79**, 044911 (2009); Phys. Rev. C **80**, 014906 (2009); arXiv:0910.2666 [nucl-th]; arXiv:0910.1548 [nucl-th]; arXiv:0909.4725 [nucl-th]; K. Dusling and I. Zahed, Nucl. Phys. A **833**, 172 (2010).
[8] M.H. Thoma, IEEE Trans. Plasma Science **32**, 738 (2004)
[9] A. Filinov, M. Bonitz, and W. Ebeling, J. Phys. A **36**, 5957 (2003).
[10] G. Kelbg, Ann. Phys. (Leipzig) **12**, 219 (1962); **13**, 354 (1963).
[11] K. Dusling and C. Young, arXiv:0707.2068 [nucl-th].
[12] A. Filinov, V. Golubnychiy, M. Bonitz, *et al.*, Phys. Rev. E **70**, 046411 (2004)
[13] M. Bonitz, A. Filinov, V. Golubnychyi, *et al.*, J. Phys. A **36**, 5921 (2003); Phys. **15**, 055704 (2008).
[14] V. S. Filinov, M. Bonitz, W. Ebeling, and V. E. Fortov, Plasma Phys. Control. Fusion **43**, 743 (2001).
[15] V. S. Filinov, M. Bonitz, and V. E. Fortov, JETP Lett. **72**, 245 (2000).
[16] M. Bonitz, V. S. Filinov, V. E. Fortov., *et al.*, Phys. Rev. Lett. **95**, 235006 (2005).
[17] V. S. Filinov, M. Bonitz, P. R. Levashov, *et al.*, J. Phys. A **36**, 6069 (2003).
[18] M. Bonitz, V. S. Filinov, V. E. Fortov, *et al.*, J. Phys. A **39**, 4717 (2006).
[19] V. S. Filinov, H. Fehske, M. Bonitz, *et al.*, Phys. Rev. E **75** , 036401 (2007).
[20] V.S. Filinov, M. Bonitz, Yu. B. Ivanov, *et al.*, Contrib. Plasma Phys., **49**, 536 (2009).
[21] V.S. Filinov, M. Bonitz, Yu. B. Ivanov, *et al.*, e-Print: arXiv:1006.3390 [nucl-th].
[22] P. Petreczky, F. Karsch, E. Laermann, *et al.*, Nucl. Phys. Proc. Suppl. **106**, 513 (2002).
[23] J. Liao and E. V. Shuryak, Phys. Rev. D **73**, 014509 (2006).
[24] S. K. Wong, Nuovo Cimento A **65**, 689 (1970).
[25] J. L. Richardson, Phys. Lett. B **82**, 272 (1979).
[26] R. P. Feynman, and A. R. Hibbs, *Quantum Mechanics and Path Integrals* (McGraw-Hill, New York, 1965).
[27] V. M. Zamalin, G. E. Norman, and V. S. Filinov, *The Monte Carlo Method in Statistical Thermodynamics* (Nauka, Moscow, 1977), (in Russian).
[28] A. V. Filinov, V. S. Filinov, Yu. E. Lozovik and M. Bonitz, *Introduction to Computational Methods for Many-Body Physics*, Ed. by M. Bonitz and D. Semkat (Rinton Press, Princeton, 2006).
[29] V. S. Filinov, M. Bonitz, Y.B. Ivanov, V.V. Skokov, P.R. Levashov, and V.E. Fortov, Contrib. Plasma. Phys. **51**, N4, 322-327 (2011).